




Two 2-fold interpenetrated polythreading networks assembled by 4,4'-sulfonyldibenzoic acid and N-donor ligand

Yan Wang, Song-Quan Shen, Ju-Hong Zhou, Dan Li, Jing Zhou, Meng Ye, Xiao-Xiao Wang, Guang-Xiang Liu & Tao Wang

To cite this article: Yan Wang, Song-Quan Shen, Ju-Hong Zhou, Dan Li, Jing Zhou, Meng Ye, Xiao-Xiao Wang, Guang-Xiang Liu & Tao Wang (2015) Two 2-fold interpenetrated polythreading networks assembled by 4,4'-sulfonyldibenzoic acid and N-donor ligand, Journal of Coordination Chemistry, 68:10, 1676-1687, DOI: [10.1080/00958972.2015.1026264](https://doi.org/10.1080/00958972.2015.1026264)

To link to this article: <http://dx.doi.org/10.1080/00958972.2015.1026264>

 View supplementary material 

 Accepted author version posted online: 17 Mar 2015.
Published online: 01 Apr 2015.

 Submit your article to this journal 

 Article views: 75

 View related articles 

 View Crossmark data 

Two 2-fold interpenetrated polythreading networks assembled by 4,4'-sulfonyldibenzoic acid and N-donor ligand

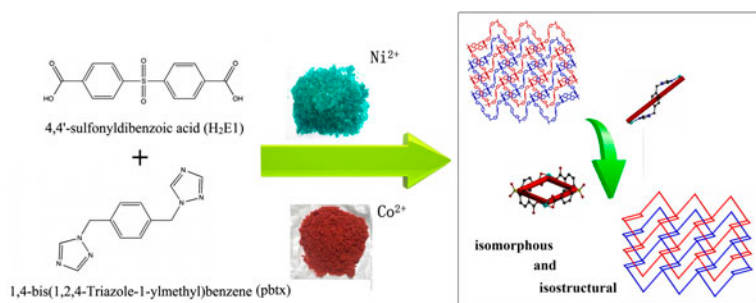
YAN WANG^{†,‡}, SONG-QUAN SHEN[†], JU-HONG ZHOU^{*†}, DAN LI[†], JING ZHOU[†], MENG YE[†], XIAO-XIAO WANG[†], GUANG-XIANG LIU[§] and TAO WANG[†]

[†]School of Chemistry and Chemical Engineering, Anhui Key Laboratory of Functional Coordination Compounds, Anqing Normal University, Anqing, China

[‡]State Key Laboratory of Coordination Chemistry, Nanjing University, Nanjing, China

[§]School of Biochemical and Environmental Engineering, Nanjing Xiaozhuang University, Nanjing, China

(Received 7 May 2014; accepted 23 February 2015)



Two 2-fold interpenetrated polythreading networks, $[\{Ni(pbtX)(E1)(H_2O)\} \cdot H_2O]_n$ (**1**) and $[\{Co(pbtX)(E1)(H_2O)\} \cdot H_2O]_n$ (**2**), were constructed by aromatic polycarboxylic acid H_2E1 ($H_2E1 = 4,4'$ -sulfonyldibenzoic acid) and $pbtX$ ($pbtX = 1,4$ -bis(1,2,4-triazole-1-ylmethyl)benzene). **1** and **2** show distinctive new interpenetrated structure of two identical single nets interlocked with each other via rotaxane-like links.

Self-assembly of Ni^{II}/Co^{II} with 4,4'-sulfonyldibenzoic acid (H_2E1) and 1,4-bis(1,2,4-triazole-1-ylmethyl)benzene ($pbtX$) has produced 3-D interpenetrated polythreading networks with non-trivial linkages, $[\{Ni(pbtX)(E1)(H_2O)\} \cdot H_2O]_n$ (**1**) and $[\{Co(pbtX)(E1)(H_2O)\} \cdot H_2O]_n$ (**2**), respectively. Single-crystal X-ray diffraction analyses revealed that **1** and **2** are isomorphous and isostructural. Complexes **1** and **2** possess a 2-D grid layer consisting of metal ions bridged by $pbtX$ ligands and entirely deprotonated $E1^{2-}$ ligands, which led to the formation of 2-fold interpenetrated polythreading networks. The interpenetrated networks were further bridged by $C-H \cdots O$ and $O-H \cdots O$ hydrogen bonds to generate their 3-D frameworks. Further characterizations including elemental analysis, FT-IR, XPRD, and Thermogravimetric analysis have been studied.

Keywords: Interpenetrated polythreading; Coordination polymer; Crystal structure; Dual-ligand system

*Corresponding author. Email: zhoujh@aqtc.edu.cn

1. Introduction

The potential applications of coordination polymers (CPs) in porous materials, microelectronics, nonlinear optics, and catalysis with their intriguing topologies and entanglement motifs have triggered the current interest [1]. Entanglement of CPs has yielded much insight into the development of structural modulation [2] and has become a promising means to synthesize new materials [3]. Interpenetration has always been the major investigated type of entanglement [4]. The increasing number of CPs reported has led to recognition of more complex types of entanglement [5]. Appropriate organic ligands and metal ions are crucial to design and synthesize target CPs [6–8], determining their structures, dimensionality, potential properties, and applications [9–13]. Due to these differences, complex entanglements have three distinguishing shapes: polycatenation, polythreaded, and polyknotting [5b]. The polycatenation has been observed with a higher dimensionality than interpenetration of component motifs, while the polythreaded structures are characterized by the presence of closed loops. The polyknotting is typical of self-penetrating nets [14].

We target polythreading CPs through dual-ligand systems containing kinked or longer co-ligands because of the looped motifs or large cavities thus formed which allow other ligands to penetrate [15]. Here, we reported two interpenetrated two-dimensional metal–organic framework structures, Ni(pbtx)(E1)(H₂O)₂ (**1**) and Co(pbtx)(E1)(H₂O)₂ (**2**), with the same aromatic carboxylic acid H₂E1 (H₂E1 = 4,4'-sulfonyldibenzoic acid) and ligand pbtx (pbtx = 1,4-bis(1,2,4-triazole-1-ylmethyl)benzene). The pbtx possesses the merits of triazole which can coordinate with the metal ions in various modes. In addition, its –CH₂– spacer allowed the phenylene ring and triazole ring with flexible conformations and better adaptability to construct polymeric networks [16]. By varying the metal nodes, we obtain two 2-D polythreading CPs with the same metal-to-ligand ratio. Herein, we investigate their structural diversities and non-trivial linkages.

2. Experimental

2.1. Materials

2.1.1. Materials and physical measurements. Commercially available reagents were used as received without further purification. The ligand pbtx was prepared based on reported procedures [17].

2.2. Synthesis of complexes

2.2.1. Synthesis of $\{[\text{Ni}(\text{pbtx})(\text{E1})(\text{H}_2\text{O})]\cdot\text{H}_2\text{O}\}_n$ (1**).** A mixture of Ni(NO₃)₂·6H₂O (29.1 mg, 0.1 mmol), H₂E1 (30.4 mg, 0.1 mmol), Na₂CO₃ (10.6 mg, 0.1 mmol), and pbtx (24.0 mg, 0.1 mmol) was dissolved in 10 mL of distilled water. The final mixture was sealed in a 15 mL Parr Teflon-lined stainless-steel vessel and heated at 140 °C for three days, and then the reaction system was cooled to room temperature. Green crystals were obtained in 56% (35.8 mg) yield (based on Ni). Elemental analysis (EA) (%) Calcd for (C₂₆H₂₄N₆Ni₁O₈S₁): C, 48.84; N, 13.14; H, 3.75. Found: C, 48.77; N, 13.25; H, 3.61. FT-IR(KBr, cm⁻¹): 3379(br), 3114(w), 1601(m), 1550(m), 1396(s), 1280(m), 1166(m), 1010(m), 866(w), 744(s), 677(m), 616(m), 488(w).

2.2.2. Synthesis of $\{[Co(pbtX)(E1)(H_2O)] \cdot H_2O\}_n$ (2**).** A mixture of $Co(NO_3)_2 \cdot 6H_2O$ (29.1 mg, 0.1 mmol), H_2E1 (30.4 mg, 0.1 mmol), Na_2CO_3 (10.6 mg, 0.1 mmol), and pbtX (24.0 mg, 0.1 mmol) was dissolved in 10 mL of distilled water. The final mixture was sealed in a 15 mL Parr Teflon-lined stainless-steel vessel and heated at 140 °C for three days, and then the reaction system was cooled to room temperature. Purple crystals were obtained in 56% (36.1 mg) yield (based on Co). EA (%) Calcd for $(C_{26}H_{24}N_6Co_1O_8S_1)$: C, 48.83; N, 13.14; H, 4.07. Found: C, 48.93; N, 13.27; H, 3.98. FT-IR(KBr, cm^{-1}): 3449(br), 3148(w), 1595(m), 1544(m), 1393(s), 1278(m), 1166(m), 1018(w), 857(w), 748(s), 677(w), 615(w), 490(w).

2.3. Physical measurements and X-ray structural determination

EA for C, H, and N were performed on an Elementar Vario EL-III elemental analyzer. Infrared spectra were performed on a Nicolet AVATAR-350 spectrophotometer with KBr pellets from 400 to 4000 cm^{-1} . UV-vis absorption spectra with KBr as background were recorded on a Shimadzu Uv-2550 spectrophotometer. Powder X-ray diffraction patterns were recorded on a Rigaku D/max-RA rotating anode X-ray diffractometer with graphite monochromated Cu-K α ($\lambda = 1.542 \text{ \AA}$) radiation at room temperature. Thermal gravimetric analysis (TGA) was performed on a Netzsch STA-409PC instrument in flowing N_2 with a heating rate of 20 °C/min. All measurements were carried out under the same experimental conditions.

Table 1. Crystal data and structure refinements for **1** and **2**.

	1	2
Empirical formula	$C_{26}H_{24}N_6NiO_8S$	$C_{26}H_{24}N_6CoO_8S$
Formula weight	639.280	639.500
Temperature (K)	298(2)	298(2)
Crystal system	Triclinic	Triclinic
Space group	P $\bar{1}$	P $\bar{1}$
<i>a</i> (Å)	10.0794(5)	10.0623(4)
<i>b</i> (Å)	10.9385(5)	11.0388(5)
<i>c</i> (Å)	13.1424(6)	13.1432(6)
α (°)	71.24(0)	70.99(0)
β (°)	88.18(0)	88.72(0)
γ (°)	76.72(0)	76.56(0)
<i>V</i> (Å ³)	1333.93(117)	1340.22(121)
<i>Z</i>	2	2
<i>D</i> _c (g·cm ⁻³)	1.592	1.585
Absorption coefficient (mm)	0.869	0.781
θ range (°)	1.64–25.00	1.64–27.53
Limiting indices	$-11 \leq h \leq 11, -13 \leq k \leq 13,$ $-15 \leq l \leq 15$	$-13 \leq h \leq 13, -14 \leq k \leq 14,$ $-17 \leq l \leq 17$
<i>F</i> (0 0 0)	660	658
Reflections collected	14,137	19,816
Unique reflections	4646 [<i>R</i> _{int} = 0.0637]	6117 [<i>R</i> _{int} = 0.0714]
Reflections observed [<i>I</i> > 2 σ (<i>I</i>)]	4209	5438
Data/restraints/parameters	4646/2/387	6117/2/387
Goodness-of-fit on <i>F</i> ²	1.007	1.048
<i>R</i> ₁ , <i>wR</i> ₂ [<i>I</i> > 2 σ (<i>I</i>)]	0.0449, 0.1309	0.0419, 0.1224
<i>R</i> ₁ , <i>wR</i> ₂ (all data)	0.0500, 0.1347	0.0468, 0.1272
Largest diff. peak and hole (e ⁻ ·Å ⁻³)	1.267, -0.654	1.284, -0.423

Table 2. Selected bond lengths (Å) and angles (°) for **1** and **2**.

Complex 1			
Ni1–O3	2.045(2)	Ni1–O5 ⁱ	2.084(2)
Ni1–O1W	2.046(2)	Ni1–O6 ⁱ	2.227(2)
Ni1–N3	2.073(3)	Ni1–N6	2.080(3)
O3–Ni1–O1W	92.93(10)	O1W–Ni1–O6 ⁱ	157.15(9)
O3–Ni1–N3	87.92(11)	N3–Ni1–O6 ⁱ	112.12(10)
O1W–Ni1–N3	90.72(11)	N6–Ni1–O6 ⁱ	87.89(10)
O3–Ni1–N6	174.14(10)	O5 ⁱ –Ni1–O6 ⁱ	60.90(8)
O1W–Ni1–N6	92.8(1)	N3–Ni1–O5 ⁱ	172.22(10)
N3–Ni1–N6	90.76(11)	N6–Ni1–O5 ⁱ	92.33(10)
O3–Ni1–O5 ⁱ	88.30(9)	O3–Ni1–O6 ⁱ	87.32(9)
O1W–Ni1–O5 ⁱ	96.26(9)		
Complex 2			
Co1–O1W	2.0654(16)	Co1–O1	2.1353(16)
Co1–O3 ⁱ	2.0792(16)	Co1–N3	2.1386(18)
Co1–N6	2.113(2)	Co1–O2	2.2549(17)
O1W–Co1–O3 ⁱ	92.11(7)	N6–Co1–N3	90.27(8)
O1W–Co1–N6	93.13(8)	O1–Co1–N3	92.95(7)
O3 ⁱ –Co1–N6	87.63(8)	O1W–Co1–O2	153.56(7)
O1W–Co1–O1	93.89(7)	O3 ⁱ –Co1–O2	88.56(7)
O3 ⁱ –Co1–O1	88.57(7)	N6–Co1–O2	113.30(7)
N6–Co1–O1	172.14(7)	O1–Co1–O2	59.70(6)
O1W–Co1–N3	92.58(7)	N3–Co1–O2	88.06(7)
O3 ⁱ –Co1–N3	174.96(7)		

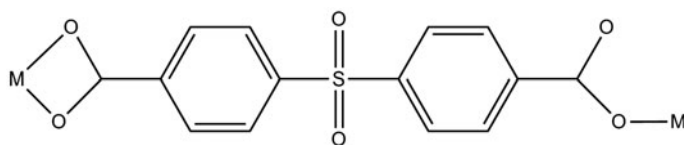
Note: Symmetry codes for **1**: (i) 1 – x, –y, 1 – z; (ii) 1 – x, 2 – y, 1 – z; (iii) 2 – x, 2 – y, –z; for **2**: (i) 1 – x, 2 – y, 1 – z; (ii) –x, –y, 2 – z; (iii) 1 – x, –y, 1 – z.

2.3.1. X-ray crystallography. X-ray diffraction data were collected on a Bruker Smart Apex II CCD equipped with a Mo-K α radiation ($\lambda = 0.71073$ Å). The data were integrated by using SAINT [18], which was also used for intensity corrections for Lorentz and polarization effects. An empirical absorption correction was applied using SADABS [19]. The structures were solved by direct methods with SHELXS-97 and refined with SHELXL-97 by full-matrix least-squares on F^2 . Hydrogens of O1W were located from the electron density map, while hydrogens of O2W were generated according to the chemical environment and formations of hydrogen bond interactions. Other hydrogens were generated geometrically. All non-hydrogen atoms were refined anisotropically and hydrogens, isotropically. All calculations were performed on a personal computer with the SHELXL-97 crystallographic software package [20]. Details of the crystal parameters, data collection, and refinement for the compounds are summarized in table 1. Selected bond lengths and angles with their estimated standard deviations are listed in table 2.

3. Results and discussion

3.1. Crystal structure

Single-crystal X-ray structural analysis revealed that [$\{\text{Ni}(\text{pbtx})(\text{E1})(\text{H}_2\text{O})\} \cdot \text{H}_2\text{O}\}_n$ (**1**) and [$\{\text{Co}(\text{pbtx})(\text{E1})(\text{H}_2\text{O})\} \cdot \text{H}_2\text{O}\}_n$ (**2**) are isomorphous and isostructural with the same space group $P\bar{1}$ as listed in table 1 with the results of crystallographic analysis. Thus, only the structure of **1** is presented here as an illustration. The asymmetric unit of **1** consists of one

Scheme 1. Coordination modes of $E1^{2-}$.

Ni^{II} , one pbtx, one carboxylic acid, one coordinated water, and one lattice water. Each Ni^{II} ion is $\{NiN_2O_4\}$ six-coordinate with a distorted octahedral environment in which the equatorial coordination sites are occupied by N3 from one pbtx ligand with an Ni–N3 bond length of 2.073(3) Å and three oxygens (O5, O6, and O1W) from the carboxylate groups of an $E1^{2-}$ ligand and one water (scheme 1). The axial position is occupied by O3 and N6 from the carboxylate unit of another $E1^{2-}$ and pbtx (Ni1–N6 = 2.080(3) Å). The structure of **1** is shown in figure 1. The Ni–O bond lengths are 2.045(2)–2.227(2) Å as listed in table 2, in which three of the Ni–O bond distances are nearly the same, but one is different. The Ni–O bond distances are in accord with the reported $\{[HPMo_{11}Ni(4,4\text{-bpy})O_{39}][Ni(4,4\text{-bpy})(H_2O)_3]\} \cdot 2(4,4\text{-Hbpy}) \cdot 3H_2O$ (bpy = bipyridine), presented by Liang and coworkers with Ni–O distances of 2.00(3)–2.22(6) Å, where six of the Ni–O bond distances are nearly the same, but one is different [21].

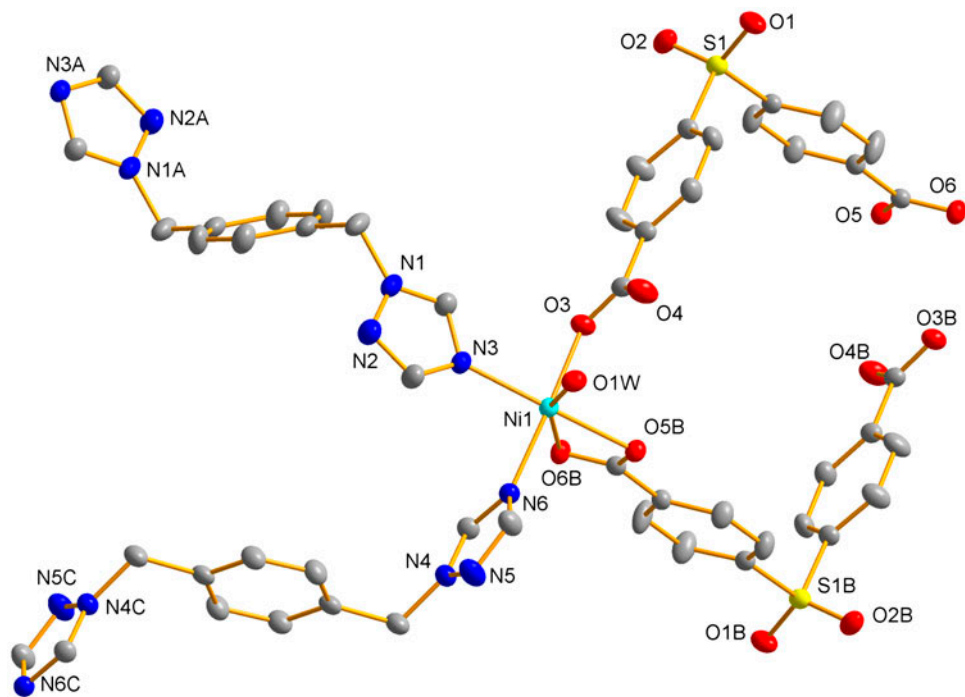


Figure 1. Single-crystal X-ray structure of **1** showing coordination environment of the $Ni(II)$ ions, where the thermal ellipsoids were drawn at the 30% probability level and lattice water molecules and hydrogens were omitted for clarity. Symmetry codes: (A) $1-x, 2-y, 1-z$; (B) $1-x, -y, 1-z$; (C) $2-x, 2-y, -z$.

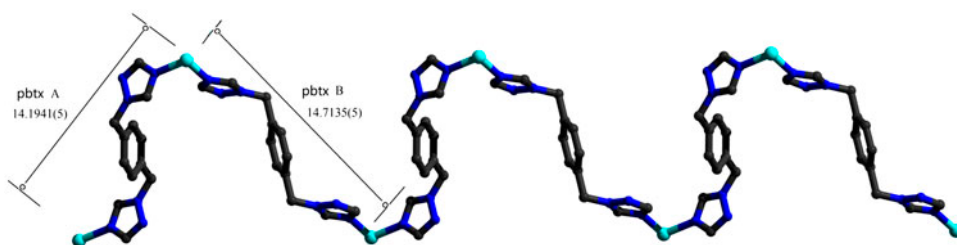


Figure 2. View of zig-zag $[\text{Ni}(\text{pbtX})]_n$ chain.

While in **2**, each Co^{II} possesses a $\{\text{CoN}_2\text{O}_4\}$ coordination environment, with two triazole nitrogen donors from two different pbtX ligands, three oxygens from two carboxylate groups of E1^{2-} ligands and one water ($\text{Co1-O1W} = 2.0654(16)$, $\text{Co1-O1} = 2.1353(16)$, $\text{Co1-O3} = 2.0792(16)$, $\text{Co1-N3} = 2.1386(18)$, $\text{Co1-N6} = 2.113(2)$, $\text{Co1-O2} = 2.2549(17)$). The Co–O distances are in agreement with the reported $\text{Co}_3(\text{bta})_2(\text{bib})_2$ ($\text{H}_3\text{bta} = 1,3,5$ -benzenetriacetic acid, $\text{bib} = 1,3$ -bis(1-imidazolyl)benzene), presented by Zhang and coworkers, where the Co–O distances varies from 1.9694(16) to 2.3991(15) Å [22].

In **1**, the Ni^{II} ions are linked by the organic ligands groups from pbtX ligands to form an infinite 1-D zigzag chain (figure 2) in which the pbtX are *trans*-conformation. The $\text{Ni}\cdots\text{Ni}$

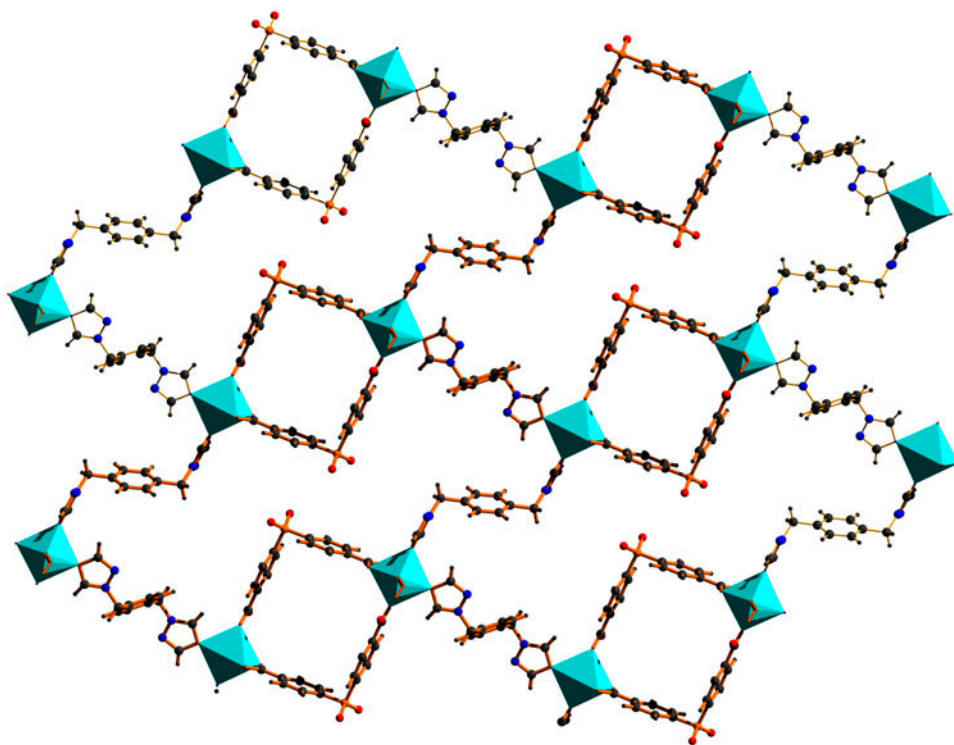


Figure 3. Polyhedral representation of the 2-D layer structure.

contact distances through the crystallographically distinct pbtX ligands are 14.19 and 14.71 Å, respectively. These differences are provided by conformational variances within the pbtX ligands. In **1**, there are two conformationally different pbtX ligands (denoted by A and B). In **1**, two triazole rings of pbtX ligands are parallel, which is a consequence of the crystal symmetry. In pbtX-A, the dihedral angle between the planes of triazole and benzene rings is 66.1°, while the corresponding dihedral angle in pbtX-B is 72.1°. These 1-D chains are further linked through E1²⁻ ligands, which lead to the formation of a 2-D network in the *bc* plane (figure 3). In **1**, each E1²⁻ links two Ni^{II} ions with its carboxylate groups adopting $\mu_1-\eta^1:\eta^1$ and $\mu_1-\eta^1:\eta^0$ coordination modes, respectively, which led to a 28-membered M₂L₂ cyclic loop with diameters of ca. 11.43 × 12.91 Å [figure 4(c)]. The apertures and Ni₂(E1)₂ loops are large enough to permit two identical single Ni(pbtX)(E1)(H₂O)₂ nets to be interlocked with each other via rotaxane-like links. As depicted in figure 4(a) and (b), the M₂L₂ loops in **1** are penetrated by pbtX ligands of a second identical lattice and *vice versa* [figure 4(a)]. In **1**, the O–O distances (e.g. O1W–O5ⁱⁱ, O1W–O4, O2W–O1ⁱ, and O2W–O6^v) of 2.566(4)–2.92(3) Å and O–H–O angles (e.g. O1W–H1WA–O5ⁱⁱ, O1W–H1WB–O4, O2W–H2WA–O1ⁱ, and O2W–H2WB–O6^v) from 166(5)° to 180° indicate formation of O–H···O hydrogen bonds between neighboring water molecules, carboxyl O, and sulfonyl O (figure 5). Furthermore, there are also C–H···O hydrogen bond interactions (C–O distances ranging from 3.092(4) to 3.428(5) Å with C–H–O angles of 131°–169°, respectively) between neighboring 2-D skeletons and water molecules (table 3). These hydrogen bonds link the 2-D sheets into a 3-D architecture.

As reported in recent literature, metal–organic framework structures assembled from 4,4-sulfonyldibenzoic acid and rod-like N-donor auxiliary ligand always have similar crystal structures [23, 24]. Hong has reported a similar complex, [$\{\text{Co}_4(\text{E}1)_4(\text{bpmp})_3(\text{H}_2\text{O})_4\} \cdot 2\text{H}_2\text{O}\}_n$ (bpmp = bis(4-pyridylmethyl)piperazine), in which Co^{II} with E1²⁻ and bpmp produced 3-D interpenetrated polythreading networks [23]. Bisht also reported similar complexes, [Co(E1)(BIX)]_n and [$\{\text{Co}(\text{E}1)(\text{bpmp})\} \cdot 2\text{H}_2\text{O}\}_n$ (BIX = 1,4-bis(imidazol-1-ylmethyl)benzene) [24], in which Co^{II} centers and entirely deprotonated E1²⁻ ligands produced similar paddle-wheel type SBU similar to **1** and **2**, demonstrating that the flexible pbtX ligands are candidates to construct coordination networks. The differences between these structures may result from the diversities of the auxiliary N-donor ligands.

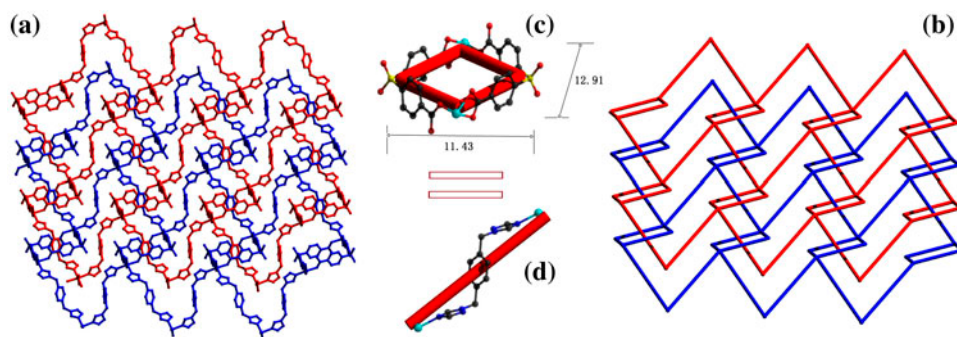


Figure 4. (a) The polythreaded (4,4) layers with 2-fold interpenetrated framework; (b) schematic perspective of the polythreaded (4,4) layers; (c) Ni₂(E1)₂ loop; (d) trans-pbtX rod in **1**.

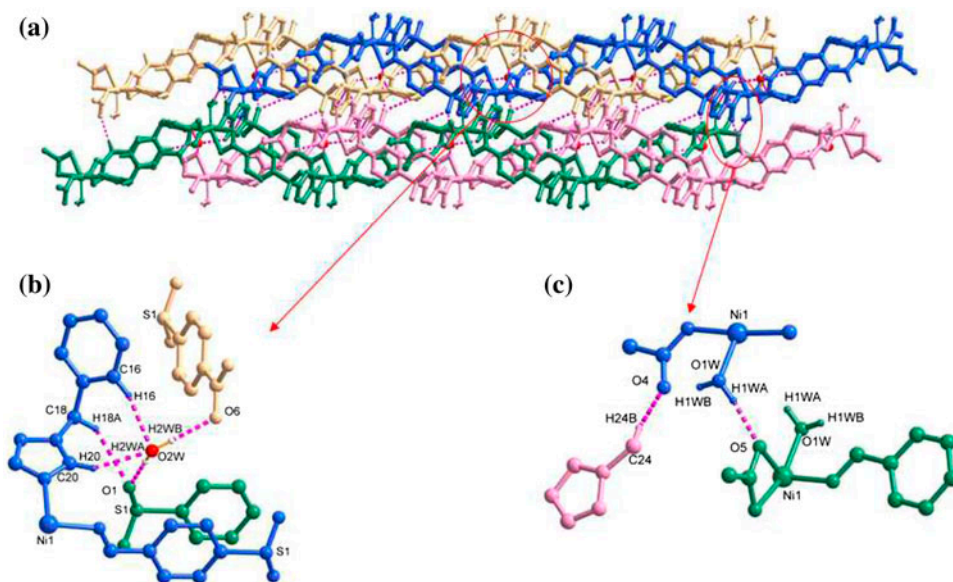


Figure 5. (a) View of **1** showing the undulating nature of the ladders which allows them to interweave in a parallel fashion. The 2-D layers are further extended to a 3-D network via intermolecular hydrogen bonds where the hydrogen bond interactions were indicated by red dashed lines. (b) H-bond (the red dotted lines) between ligand and free water molecule in **1**. (c) The intermolecular H-bond (the red dotted lines) between interlayer ligands in **1** (see <http://dx.doi.org/10.1080/00958972.2015.1026264> for color version).

Table 3. Hydrogen bond lengths (Å) and angles (°) for **1** and **2**.

D-H...A	d(D-H)	d(H...A)	d(D...A)	⟨DHA
Complex 1				
O1W-H1WA...O5 ⁱⁱ	0.84(3)	1.88(3)	2.721(3)	172(4)
O1W-H1WB...O4	0.86(5)	1.72(5)	2.566(4)	166(5)
O2W-H2WA...O1 ⁱ	0.85	2.06	2.92(3)	180
O2W-H2WB...O6 ^v	0.85	1.95	2.80(2)	179
C16-H16...O2W	0.93	2.36	3.27(3)	163
C18-H18A...O1 ⁱ	0.97	2.58	3.428(5)	146
C20-H20...O2W	0.93	2.35	3.20(2)	152
C24-H24B...O4 ^{iv}	0.97	2.33	3.285(5)	169
C26-H26...O2 ⁱⁱⁱ	0.93	2.40	3.092(4)	131
Complex 2				
O1W-H1WB...O1 ⁱⁱ	0.85(2)	1.86(2)	2.705(2)	175(3)
O1W-H1WA...O4 ⁱ	0.87(3)	1.74(3)	2.573(3)	162(4)
O2W-H2WA...O2 ^{vii}	0.85	2.02	2.78(2)	148
O2W-H2WB...O3 ^v	0.85	2.18	2.95(2)	151
C10-H10...O2W ^{iv}	0.93	2.52	3.38(2)	153
C18-H18A...O4 ⁱⁱⁱ	0.97	2.33	3.292(3)	171
C20-H20...O5 ^v	0.93	2.42	3.105(3)	131
C23-H23...O2W	0.93	2.29	3.20(2)	165
C24-H24B...O6 ^{vi}	0.97	2.58	3.432(4)	146

Notes: Symmetry codes for **1**: (i) $-x, 1-y, 1-z$; (ii) $x, 1+y, -1+z$; (iii) $1-x, 1-y, 1-z$; (iv) $1+x, y, z$; (v) $x, 1+y, z$; for **2**: (i) $1-x, 2-y, 1-z$; (ii) $1-x, 1-y, 2-z$; (iii) $-x, 2-y, 1-z$; (iv) $x, 1+y, z$; (v) $x, -1+y, z$; (vi) $1+x, -1+y, z$; (vii) $1-x, 1-y, 1-z$.

Although Co complexes with very similar 2-D sheet structures reported by Hong and Bisht are all made with E1 and bmpm, the different coordination environments around Co^{II} and amount of solvent molecules lead to various final frameworks. The diversity of Hong and Bisht's complexes may be attributed to the synthetic conditions, including material ratio, temperature (120 °C for Hong's and 125 °C for Bisht's), and reaction time (72 h for Hong's and 97 h for Bisht's).

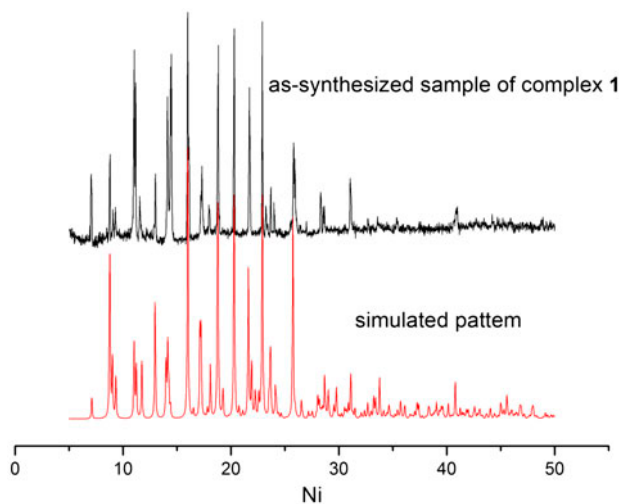


Figure 6. The simulated (red) and experimental (black) PXRD of **1** (see <http://dx.doi.org/10.1080/00958972.2015.1026264> for color version).

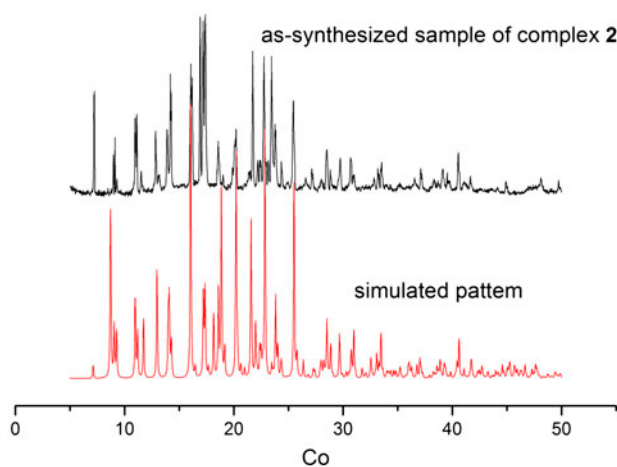


Figure 7. The simulated (red) and experimental (black) PXRD of **2** (see <http://dx.doi.org/10.1080/00958972.2015.1026264> for color version).

3.2. PXRD, TGA, and FT-IR

The homogeneities of **1** and **2** are confirmed by X-ray powder diffraction analyses (figures 6 and 7). Despite a few unindexed diffraction lines and some lightly broadened peaks, the experimental patterns of the as-synthesized samples are consistent with those calculated from X-ray single-crystal diffraction data. The difference in intensity may be due to the preferred orientation of the microcrystalline powder samples.

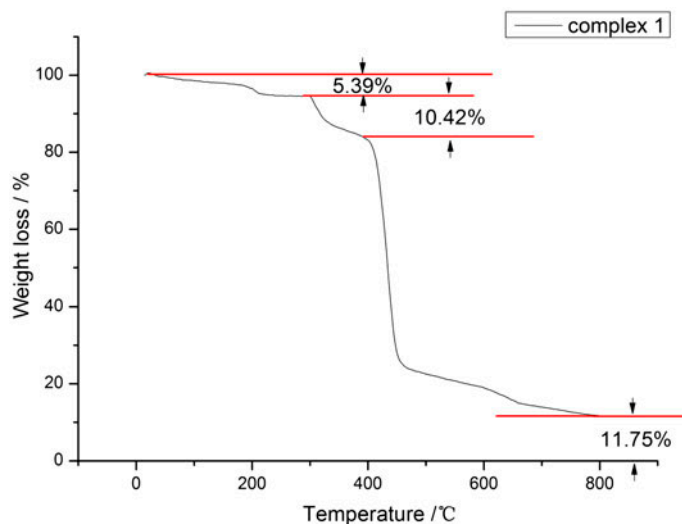


Figure 8. Thermogravimetric diagram of **1**.

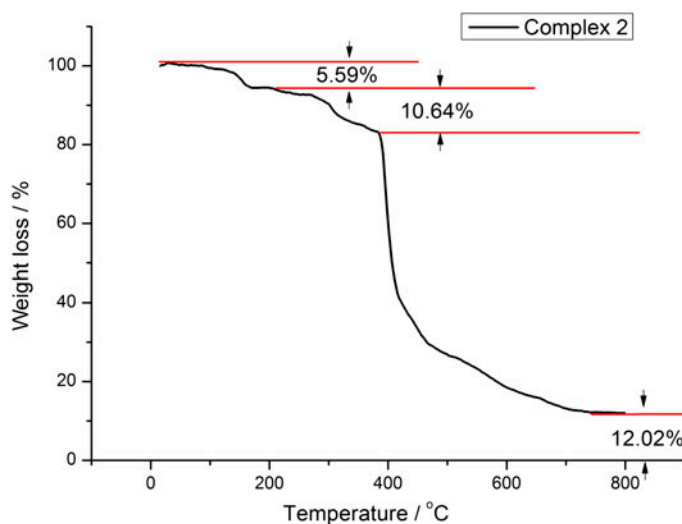


Figure 9. Thermogravimetric diagram of **2**.

Thermogravimetric diagrams (figures 8 and 9) of **1** and **2** had similar data and the results show that the weights of **1** and **2** are stable in air at ambient temperature, making them potential candidates for applications. For **1**, the TGA demonstrates that a weight loss of 5.39% starting from room temperature to 301 °C corresponds to the release of two water molecules (calculated 5.63%). The next weight loss of 10.42% at 388 °C corresponds to the collapse of the framework and release of SO₂ gas (calculated 10.00%). Its final mass remnant at 770 °C was 11.75%, consistent with deposition of NiO (calculated 11.68%). Compound **2** also undergoes dehydration from room temperature to 208 °C, as evidenced by a mass loss of 5.59% corresponding to release of water molecules (calculated 5.63%). The organic ligands were ejected at above 258 °C and SO₂ gasses were released (loss of 10.64%, calculated 10.00%). Its final mass remnant at 730 °C was 12.02%, consistent with a mixture of CoO (calculated 11.71%) and Co₂O₃ (calculated 12.96%).

No bands at 1700 cm⁻¹ were found in the IR spectra of **1** and **2**, indicating complete deprotonation of the carboxylic acid ligands, which is also consistent with the X-ray single crystallographic analysis. Strong absorptions between 1396 and 1601 cm⁻¹ in the IR can be assigned to coordinated carboxylate groups.

4. Conclusion

We presented two interpenetrated transition metal–organic framework structures based on V-shape polycarboxylate ligand and flexible N-donor auxiliary ligands, providing the necessary constituent motifs to form polythreading. The structures of our compounds demonstrate that the functionality of the building block used in network construction can be employed to control overall structure of the array instead of metal ions. Procedures to form similarly intriguing aspects of polythreading structural chemistry are still undergoing.

Supplementary material

FT-IR and UV–vis spectra of **1** and **2**. CCDC 990808 and 990809 contain the supplementary crystallographic data for **1** and **2**. These data can be obtained free of charge from the Cambridge Crystallographic Data Center via www.ccdc.cam.ac.uk/data_request/cif.

Disclosure statement

No potential conflict of interest was reported by the authors.

Funding

This work was supported by the Provincial Natural Science Foundation of Anhui [grant number 1408085QB32]; the Key Project of Anhui Provincial Fund for Distinguished Young Scholars in Colleges and Universities [grant number 2013SQRL059ZD]; and the Natural Science Foundation of Anhui Education Committee [grant number KJ2013B126].

Supplementary data

Supplemental data for this article can be accessed here [<http://dx.doi.org/10.1080/00958972.2015.1026264>].

References

- [1] (a) B. Moulton, M.J. Zaworotko. *Chem. Rev.*, **101**, 1629 (2001); (b) O.R. Evans, W. Lin. *Acc. Chem. Res.*, **35**, 511 (2002); (c) C. Janiak. *Dalton Trans.*, **14**, 2781 (2003); (d) S. Kitagawa, R. Kitaura, S.I. Noro. *Angew. Chem.*, **116**, 2388 (2004); *Angew. Chem. Int. Ed.*, **43**, 2334 (2004); (e) C.N.R. Rao, S. Natarajan, R. Vaidhyanathan. *Angew. Chem.*, **116**, 1490 (2004); *Angew. Chem. Int. Ed.*, **43**, 1466 (2004); (f) N.W. Ockwig, O. Delgado-Friedrichs, M. O'Keeffe, O.M. Yaghi. *Acc. Chem. Res.*, **38**, 176 (2005).
- [2] (a) S.R. Batten, R. Robson. *Angew. Chem. Int. Ed.*, **37**, 1460 (1998); (b) A.J. Blake, N.R. Champness, P. Hubberstey, W.-S. Li, M.A. Withersby, M. Schröder. *Coord. Chem. Rev.*, **183**, 117 (1999); (c) L. Carlucci, G. Ciani, D.M. Proserpio. *Coord. Chem. Rev.*, **246**, 247 (2003); (d) R.L. LaDuca. *Coord. Chem. Rev.*, **253**, 1759 (2009).
- [3] (a) S. Ma, D. Sun, M. Ambrogio, J.A. Fillinger, S. Parkin, H.-C. Zhou. *J. Am. Chem. Soc.*, **129**, 1858 (2007); (b) O. Shekiah, H. Wang, M. Paradinas, C. Ocal, B. Schüpbach, A. Terfort, D. Zacher, R.A. Fischer, C. Wöll. *Nat. Mater.*, **8**, 481 (2009); (c) D.-R. Xiao, D.-Z. Sun, J.-L. Liu, G.-J. Zhang, H.-Y. Chen, J.-H. He, S.-W. Yan, R. Yuan, E.-B. Wang. *Eur. J. Inorg. Chem.*, **24**, 3656 (2011); (d) B. Xu, X. Lin, Z. He, Z. Lin, R. Cao. *Chem. Commun.*, **47**, 3766 (2011).
- [4] (a) S.R. Batten, R. Robson. *Angew. Chem.*, **110**, 1558 (1998); *Angew. Chem. Int. Ed.*, **37**, 1460 (1998); (b) S.R. Batten. *CrystEngComm*, **3**, 67 (2001).
- [5] (a) L. Carlucci, G. Ciani, D.M. Proserpio. *Coord. Chem. Rev.*, **246**, 247 (2003); (b) L. Carlucci, G. Ciani, D.M. Proserpio. *CrystEngComm*, **5**, 269 (2003).
- [6] S.W. Keller. *Angew. Chem. Int. Ed. Engl.*, **36**, 247 (1997).
- [7] J. Li, H. Zeng, J. Chen, Q. Wang, X. Wu. *Chem. Commun.*, **13**, 1213 (1997).
- [8] L.-J. Zhang, J.-Q. Xu, Z. Shi, X.-L. Zhao, T.-G. Wang. *J. Solid State Chem.*, **173**, 32 (2003).
- [9] D. Sun, R. Cao, Y. Liang, Q. Shi, W. Su, M. Hong. *J. Chem. Soc., Dalton Trans.*, **16**, 2335 (2001).
- [10] (a) C. Janiak. *Dalton Trans.*, **14**, 2781 (2003); (b) S.L. James. *Chem. Soc. Rev.*, **32**, 276 (2003).
- [11] S.-L. Zheng, X.-M. Chen. *Aust. J. Chem.*, **57**, 703 (2004).
- [12] (a) D. Maspoch, D. Ruiz-Molina, J. Veciana. *J. Mater. Chem.*, **14**, 2713 (2004); (b) S.R. Batten, K.S. Murray. *Coord. Chem. Rev.*, **246**, 103 (2003).
- [13] L.-J. Zhang, J.-Q. Xu, Z. Shi, X.-L. Zhao, T.-G. Wang. *J. Solid State Chem.*, **173**, 32 (2003).
- [14] X.L. Wang, C. Qin, E.B. Wang, Y.G. Li, Z.M. Su, L. Xu, L. Carlucci. *Angew. Chem. Int. Ed.*, **44**, 5824 (2005).
- [15] (a) H. Chen, D. Xiao, L. Fan, J. He, S. Yan, G. Zhang, D. Sun, Z. Ye, R. Yuan, E. Wang. *CrystEngComm*, **13**, 7098 (2011); (b) H. Chen, D. Xiao, J. He, Z. Li, G. Zhang, D. Sun, R. Yuan, E. Wang, Q.-L. Luo. *CrystEngComm*, **13**, 4988 (2011).
- [16] (a) D. Maspoch, D. Ruiz-Molina, J. Veciana. *J. Mater. Chem.*, **14**, 2713 (2004); (b) S.R. Batten, K.S. Murray. *Coord. Chem. Rev.*, **246**, 103 (2003); (c) L. Carlucci, G. Ciani, D.M. Proserpio. *Coord. Chem. Rev.*, **246**, 247 (2003).
- [17] H.-F. Zhu, J. Fan, T. Okamura, W.-Y. Sun, N. Ueyama. *Cryst. Growth Des.*, **5**, 289 (2005).
- [18] SAINT. (*Version 6.02a*), Bruker AXS Inc., Madison, WI (2002).
- [19] G.M. Sheldrick. *SADABS, Program for Bruker Area Detector Absorption Correction*, University of Göttingen, Göttingen (1997).
- [20] (a) G.M. Sheldrick. *SHELXS-97, Program for Crystal Structure Solution*, University of Göttingen, Göttingen (1997); (b) G.M. Sheldrick. *SHELXL-97, Program for Crystal Structure Refinement*, University of Göttingen, Göttingen (1997).
- [21] J.-L. Liang, H.-J. Zhang, Y.-K. Lu, H.-L. Guo, J.-C. Zhao, M.-M. Wu, Y.-Q. Liu, C.-G. Liu. *Inorg. Chem. Commun.*, **45**, 135 (2014).
- [22] X.-D. Zhang, Y.-M. Li, L. Fan, J.-D. Pang, Z.-F. Ju. *Inorg. Chem. Commun.*, **53**, 4 (2015).
- [23] Y. Bu, F. Jiang, K. Zhou, Y. Gai, M. Hong. *CrystEngComm*, **16**, 1249 (2014).
- [24] (a) K.K. Bisht, E. Suresh. *Inorg. Chem.*, **51**, 9577 (2012); (b) K.K. Bisht, E. Suresh. *Cryst. Growth Des.*, **13**, 664 (2013).